Neuron, Volume *61*

Supplemental Data

Presynaptic Regulation of Astroglial

Excitatory Neurotransmitter Transporter GLT1

Yongjie Yang, Oguz Gozen, Andrew Watkins, Ileana Lorenzini, Angelo Lepore, Yuanzheng Gao, Svetlana Vidensky, Jean Brennan, David Poulsen, Jeong Won Park, Noo Li Jeon, Michael B. Robinson, and Jeffrey D. Rothstein

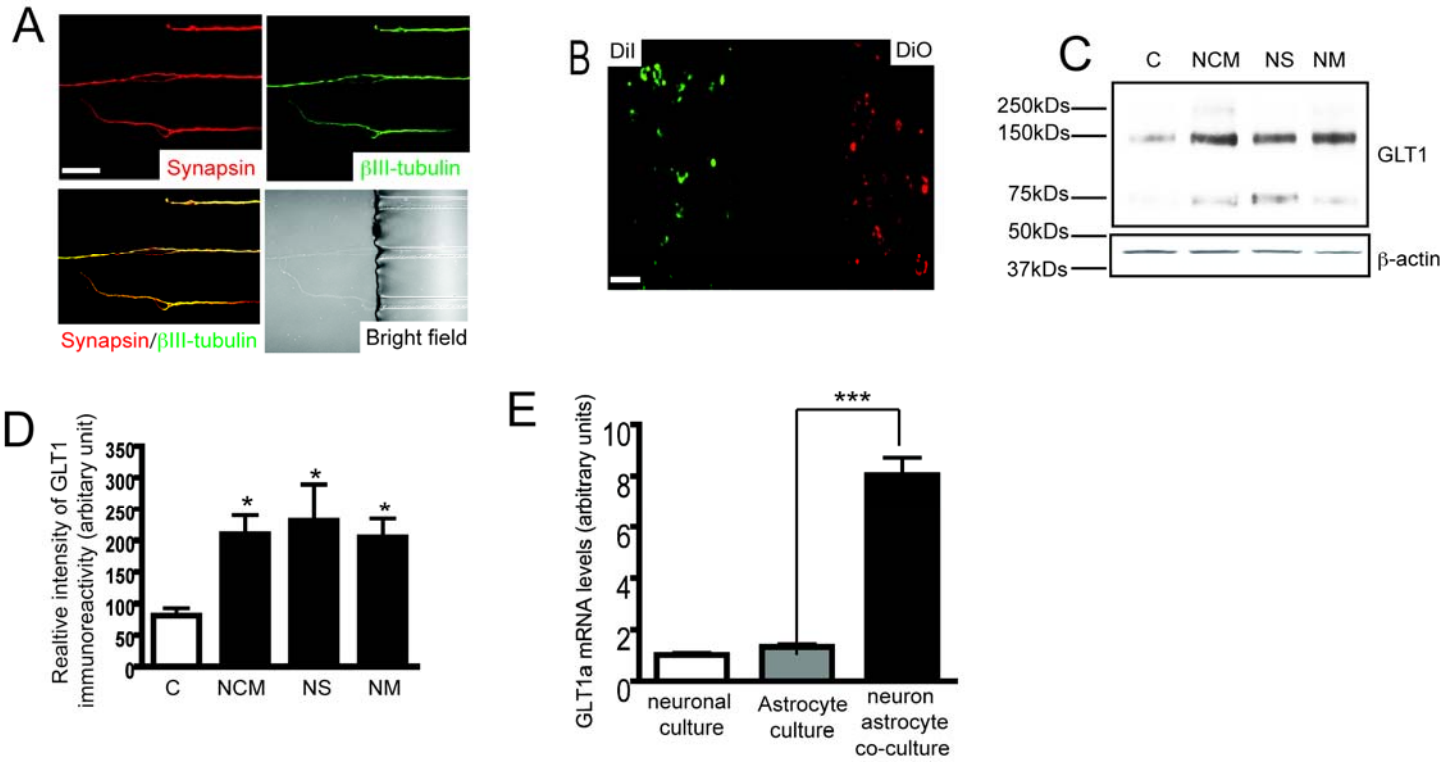

Figure S1. Neuron-dependent transcriptional activation of GLT1 in astrocytes. A. Double-labeling of synapsin-I and βIII-tubulin in MCP identifying axons. Scale bar, 20μm. **B.** Separate labeling of astroglia in MCP by DiI or DiO. Cells were examined 7 days post dye labeling; no double stained cells were observed. Scale bar, 100μm. **C.** Differential neuronal components induce GLT1 expression in cultured astrocytes. Cultured astrocytes were treated with neuron conditional medium (NCM), neuronal supernatant (NS), or neuronal membrane (NM) for 5 days. Neuronal components were collected from 7-10 day old cultured cortical neuronal cultures. For NCM, neuronal culture medium was directly collected from confluent neuronal cultures and spun down for 5min at 1000rpm to remove the cell debris; for NS and NM,

cultured neurons were resuspended in astrocyte culture medium (5-8 X 10^6 cells/ml) and lysed by Dounce homogenizer. The lysatre was then spun down to collect the supernatant (NS) and the pellet was resuspended in astrocyte culture medium as NM. **D.** Densitometric analyses of GLT1 immunoreactivity from immunoblots with neuronal component treatment (n=3). **E.** Neuron-dependent GLT1 mRNA increases in astroglia. GLT1 mRNA levels were determined by quantitative RT-PCR with mouse GLT1 specific TaqMan probe. GLT1 mRNA levels in neuronal cultures were used as calibrator for comparison (n=6) (***, $P<0.001$, one-way ANOVA and Bonferroni posthoc analysis).

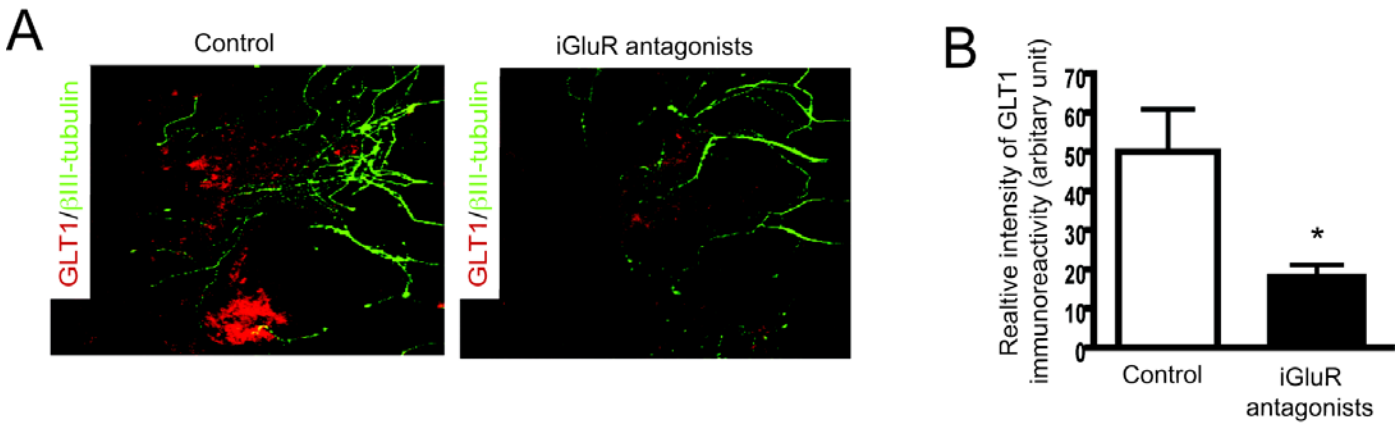

Figure S2. **Glutamate receptors contribute to neuron dependent GLT1 activation. A.** Axon-induced up-regulation of GLT1 was blocked by iGluR antagonist cocktails when added to astroglial compartment (60μM MK801 + 90μM CNQX + 300μM APV) on MCP. Scale bar, 50 μm. **B.** Quantitation of GLT1 immunoreactivity from MCP after iGluR antagonist treatment (5 astrocytes per field, 2 fields/MCP from total 3 MCPs) (Student's t-test: *, $P<0.05$).

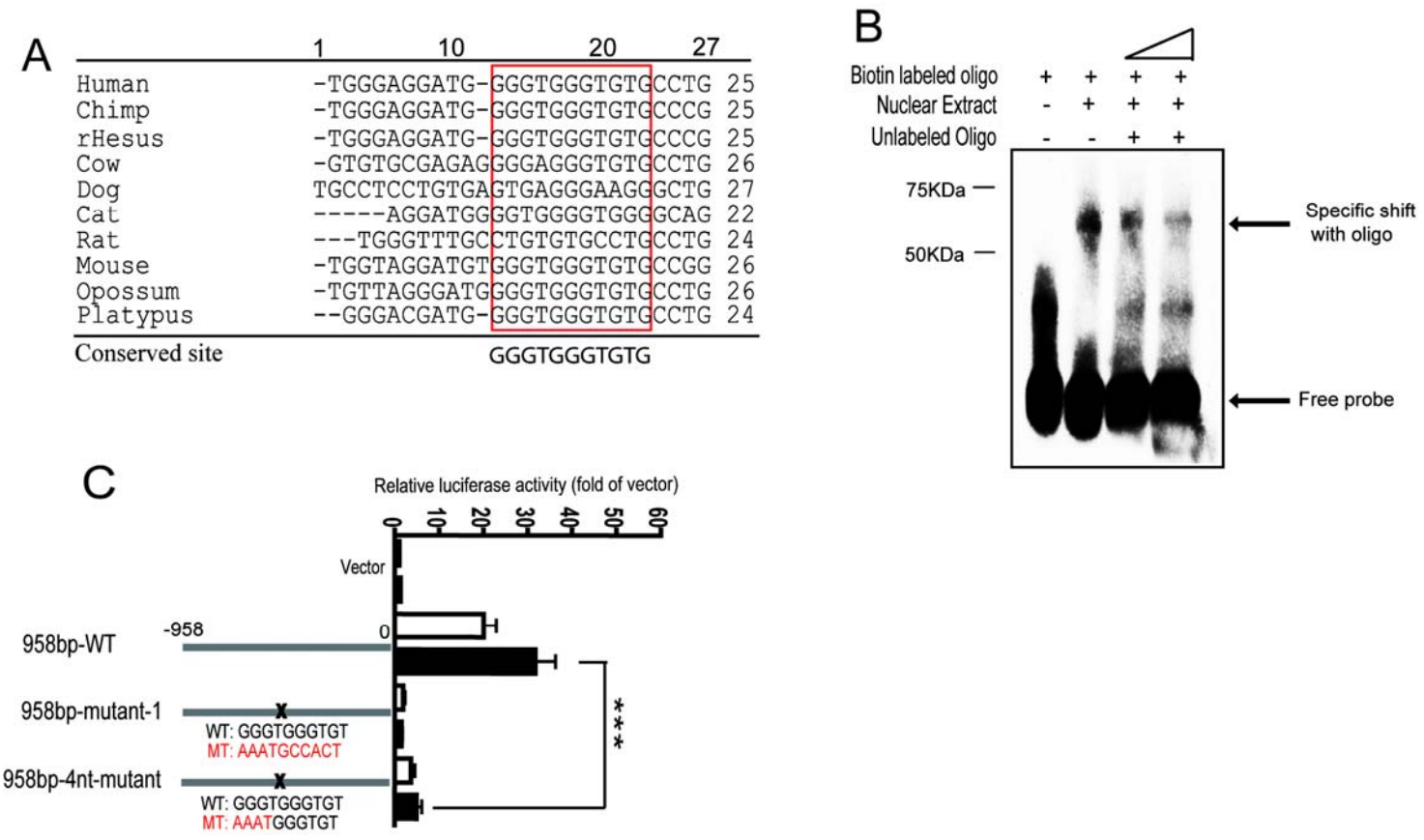

Figure S3. Characterization of the KBBP binding sequence on GLT1 promoter. A. Sequence alignment of conserved cis-element on GLT1 promoter. GLT1 promoter sequences were extracted from UCSC genome database (http://genome.ucsc.edu/cgi-bin/hgBlat) and were aligned in ClustalW2 (http://www.ebi.ac.uk/tools/clustalw2/index.html). **B.** kappa B enhancer element GGGGACTTTCC is capable of competing out GGGTGGGTGT induced specific binding in dose-dependent manner. **C.** Site-directed mutagenesis of KBBP binding sequence abolished GLT1 promoter activity in cultured astrocytes. Mutated sequences are highlighted in red (***, $P<0.001$, one-way ANOVA and Bonferroni test was used).

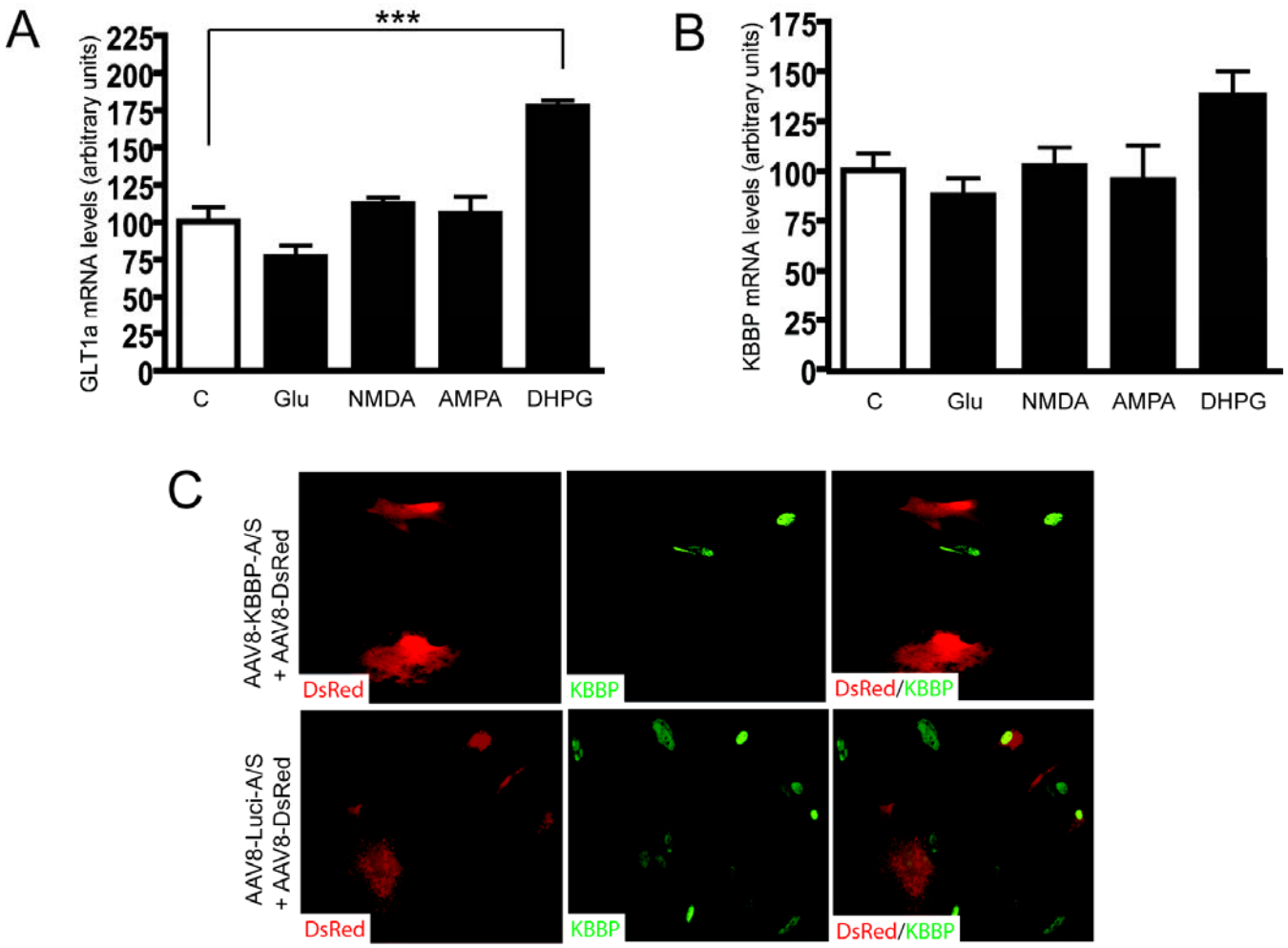

Figure S4. KBBP is essential and sufficient for neuron-dependent transactivation of GLT1. DHPG treatment increases (**A**) GLT1 mRNA levels and (**B**) KBBP mRNA levels in cultured astrocytes (n=3). Cultured astrocytes were treated with various glutamate receptor agonists (glutamate: 100 μM; NMDA: 100 μM; AMPA: 100 μM; DHPG: 50 μM) in serum-free medium for 24h. (***, $P<0.001$, one-way ANOVA and Bonferroni test). **C.** Expression of KBBP antisense decreased KBBP expression in cultured astrocytes. A/S: antisense. Cultured primary astrocytes were co-transduced with AAV8 viral particles that contain KBBP antisense or luciferase antisense (reverse sequence of cDNA) and AAV8 viral particles containing DsRed.

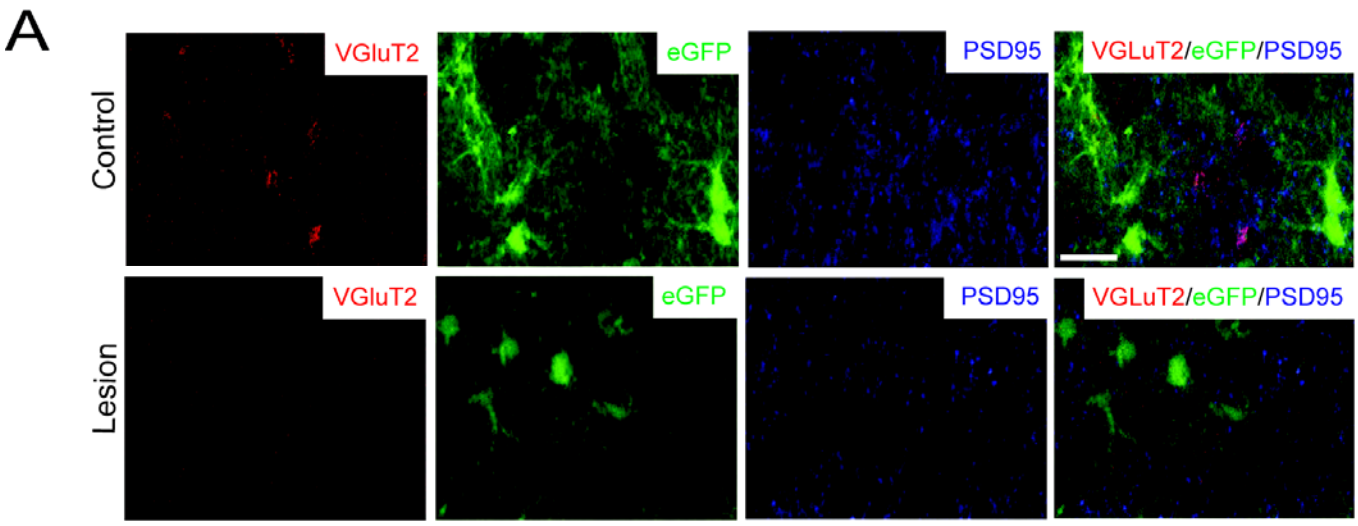

Figure S5. Spinal cord transection results in loss of pre-synaptic terminals and subsequent diminished GLT1 promoter activity. **A.** Loss of pre-synaptic terminals in transected spinal cord visualized by VGluT2 and PSD95 double staining. Reduced eGFP intensity was observed in individual astrocytes surrounding degenerated axons/pre-synaptic terminals of lesioned BAC GLT1 eGFP mice. Scale bar, 20μm.

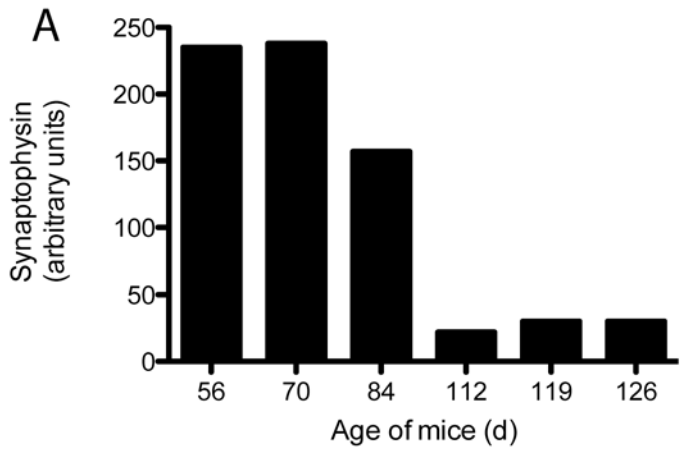

Figure S6: Dynamic changes of synaptophysin in lumbar spinal cord of SOD1 G93A mice. A. Synaptophysin protein quantification by western blot from total lumbar spinal cord of G93A mice over time. A gross loss of synaptophysin is detected prior to clinical disease onset at 90 days of age. (n=5).